

New potential candidates for astronomical searches discovered in the electrical discharge of the PAH naphthalene and acetonitrile.

Authors:

Donatella Loru^a, Amanda Steber^{a,b}, Johannes M. M. Thunnissen^c, Daniël B. Rap^c, Alexander K. Lemmens^{c,d}, Anouk M. Rijs^e and Melanie Schnell^{a,f}

^a Deutsches Elektronen-Synchrotron DESY, Notkestrasse 85, 22607 Hamburg, Germany.

^b Departamento de Química Física y Química Inorgánica, Facultad de Ciencias, Universidad de Valladolid, 47011 Valladolid, Spain

^c Radboud University, Institute of Molecules and Materials, FELIX Laboratory, Toernooiveld 7c, 6525 ED, Nijmegen, The Netherlands.

^d Van't Hoff Institute for Molecular Sciences, University of Amsterdam, Science Park 904, 1098 XH, Amsterdam, The Netherlands.

^e Division of BioAnalytical Chemistry, AIMMS Amsterdam Institute of Molecular and Life Sciences, Vrije Universiteit Amsterdam, De Boelelaan 1108, 1081 HV Amsterdam, The Netherlands.

^f Institute of Physical Chemistry, Christian-Albrechts-Universität zu Kiel, Max-Eyth-Straße 1, 24118 Kiel, Germany.

Abstract

The formation and dissociation mechanisms of polycyclic aromatic hydrocarbons (PAHs) as well as their reactivity with other interstellar molecules are elusive. In this work, we have investigated the electrical discharge chemistry of the PAH naphthalene and acetonitrile, a molecule known to be present in interstellar environments, using a combination of mass-selective IR-UV ion dip spectroscopy with the free electron laser FELIX in the mid-IR frequency region (550 – 1800 cm⁻¹), and quantum chemical calculations. In addition to the species known to be produced in the electrical discharge of pure naphthalene, $-CH_3$ and $-CN$ substituted unsaturated hydrocarbons have been identified. Most of them, in particular those containing a nitrogen atom in the molecular framework, such as benzo[7]annulene-6-carbonitrile, have a substantial dipole moment and, therefore, can be considered as potential candidates for astronomical searches. Among the species observed, the two isomers 1- and 2-cyanonaphthalene, which have been recently detected in the TMC-1, have been unambiguously identified in our experiment, thus highlighting the use of electrical discharge sources as a valuable tool to produce astronomically relevant species.

Introduction

The study of molecular infrared emission in the interstellar medium (ISM), designated as the unidentified infrared bands (UIRs), is still under way. Polycyclic aromatic hydrocarbons (PAHs), highly unsaturated carbon molecules composed of two or more fused aromatic rings, have been proposed as the potential carriers of the UIRs, thus leading some to refer to these bands also as AIBs (Aromatic Infrared bands) [1]. These bands, which are observed in the mid-IR spectral region (roughly from 3 – 20 μm) throughout the interstellar medium (ISM), are characteristic of C-H and C=C stretching and bending vibrational modes of aromatic compounds. Because of the ubiquitous nature of the UIRs, PAHs could be considered prominent members of the family of organic molecules in the ISM accounting for about 10 to 25% of the total interstellar carbon [1].

Despite the fact that the presence of PAHs has been established, the assignment of individual PAHs to the UIRs via infrared spectroscopy has not yet been possible as only broad IR have been recorded. The differences in the vibrational frequencies of these C-H and C=C vibrations between several PAHs are smaller than the width of the interstellar band profile, thereby making the disentanglement of these bands difficult. Nevertheless, very recently the presence of PAHs in the ISM has been confirmed by the first radio astronomy detection of the PAH indene and of the two carbonitrile substituted PAHs 1- and 2-cyanonaphthalene in the dark molecular cloud TMC-1 [2][3][4]. The detection of the two isomers of cyanonaphthalene is also considered as an indirect detection of the parent hydrocarbon naphthalene.

Although relevant progress has been made with the detection of indene and the two isomers of cyanonaphthalene, the role of PAHs in interstellar environments is still poorly understood. There are open questions with respect to their abundance, their formation, their reactivity, and their potential function as seeds for the formation of larger particles. Regarding their interstellar formation, two models have been proposed. On one side, there is the top-down approach, which is based on the concept that large interstellar carbon particles, such as carbon clusters or carbon soot particles, can be destroyed by the interstellar UV light to form smaller PAHs [5][6]. On the other side, there is the bottom-up approach, which postulates that PAHs can form from smaller precursors via chemical reactions, which can occur through gas-phase reactions, such as the hydrogen

abstraction-acetylene addition (HACA) mechanism [7], or via grain-surface reactions [8].

To gain insight into the formation of PAHs as well as their reactivity with cyano-containing interstellar molecules in the laboratory, we have used an electrical discharge nozzle coupled with mass-selective IR-UV ion dip spectroscopy using an infrared free electron laser [9][10]. Under plasma conditions, PAHs are expected to undergo fragmentation processes followed by recombination chemistry. The formed species can be identified via their mass in combination with their characteristic IR features in the 550 - 1800 cm^{-1} fingerprint region. Herein, we present our results obtained from electrical discharge experiments on the PAH naphthalene (C_{10}H_8) in mixture with acetonitrile (CH_3CN), a simple nitrogen-containing interstellar molecule and a source of the CN radical, also known to be abundant in several interstellar regions [11][12][13]. The plasma chemistry of the pure PAH naphthalene has been already investigated using the same experimental technique by Lemmens and coworkers [14]. In that study, new potential reaction pathways for the formation of PAHs were identified. The results of carbon insertion resulting in the formation of larger PAHs, namely phenanthrene and pyrene, were observed. Furthermore, that experiment demonstrated that, as an alternative to the HACA mechanism [7], growth of PAHs via the addition of diacetylene units should be taken into consideration.

In the experiment presented here, several new species are observed upon addition of acetonitrile. Among these are the two isomers of cyanonaphthalene, which, as mentioned, have been already detected in the TMC-1. Their observation in our experiment highlights the capability of electrical discharge sources as a powerful laboratory tool, not only to shed light on potential reaction pathways for interstellar chemistry but also to generate new species. The latter could be used as a basis for chemical investigations in TMC-1 and other interstellar clouds and could act as proxies to trace non-polar species via radioastronomy, as also discussed below.

Experimental and computational methods

The electrical discharge experiment of naphthalene and acetonitrile was performed at the FELIX laboratory using mass-selective IR-UV ion dip spectroscopy coupled with a molecular beam and an electrical discharge source [9][14]. Naphthalene (C_{10}H_8 , 99% purity) and acetonitrile (CH_3CN , 99.9 % purity)

were purchased from Sigma Aldrich and used without further purification. At room temperature, naphthalene is solid with a tabulated melting point of 80°C. To increase its gas-phase concentration, the sample was heated using a home-built heatable reservoir (to ~95 °C), directly connected to a pulsed valve (Parker Series 9 pulse valve) and positioned inside the vacuum chamber. The naphthalene/acetonitrile mixture was created by streaming argon, used as a carrier gas at a backing pressure of ca. 5 bar, first through the reservoir containing acetonitrile external to the vacuum chamber and then through the heatable reservoir containing naphthalene. After exiting the pulsed valve but before supersonic expansion, the gas pulse containing the mixture of the precursors was electrically discharged. The design of the nozzle has been thoroughly discussed in a previous publication [14], therefore only a brief description is provided here. It consists of two oxygen-free copper electrodes separated by a PEEK spacer and inserted into a PEEK housing. To increase the reaction time between the reactive species and, therefore, to favor the formation of new molecules, a 6 mm spacer was added after the two electrodes forming a recombination zone. To improve the rovibrational cooling after discharge, the final spacer was designed in a way to ensure a compression of the beam before supersonic expansion. For this experiment a voltage between 0.7 and 0.8 kV, which produced a current of about 50 mA, was found to be optimal for the formation of species having a mass-to-charge (m/z) ratio larger than the precursors (Figure 1).

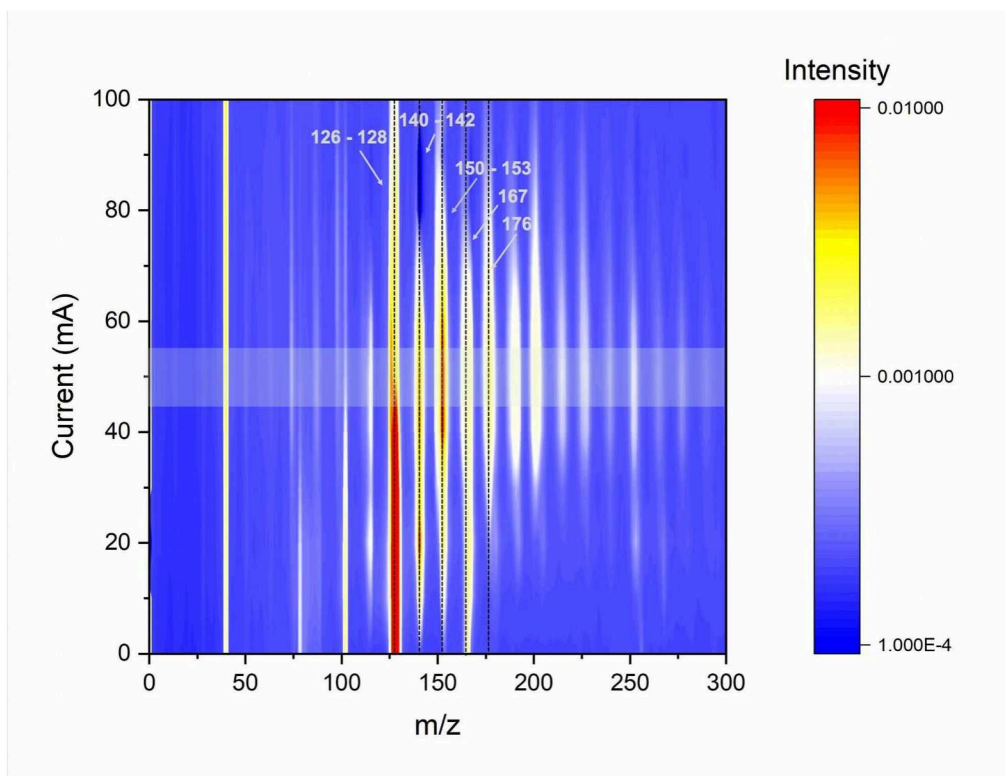


Figure 1 Discharge current vs. mass-to-charge (m/z) ratio plot showing the range of currents at which the formation of fragments or recombination species is favored. When a current of approximately 50 mA is produced, the intensity of the parent species ($m/z = 128$) decreases, whereas an increase in the intensity of most of the discharge products, as highlighted in the diagram by the white box, is observed.

At the exit of the discharge nozzle the molecular beam, containing a mixture of the carrier gas, the precursors and the newly formed species, is expanded into the vacuum chamber, skimmed and delivered internally cold to the interaction region, where it is probed using a combination of IR-UV ion dip spectroscopy and mass spectrometry. Here, the formed fragments and products present in the molecular beam are ionized using $[1 + 1']$ resonant enhanced multiphoton ionization (REMPI) with excitation by a dye laser at 275 nm and ionized with an ArF laser (193 nm). The ionized species are then mass-separated and detected using a reflectron time-of-flight spectrometer equipped with a multichannel plate ion detector. For each mass channel, an IR spectrum is recorded in the 550 – 1800 cm^{-1} fingerprint region using the IR-UV ion dip experimental scheme with the free electron laser FEL-2 at the FELIX laboratory [15].

The assignment of the IR spectra to a specific molecule was achieved by comparing the experimental IR spectra with theoretical IR spectra of possible structures. For all indicated mass channels (see Figure 2), we have optimized the structure of possible isomers with that specific mass and computed their IR spectra. The theoretical spectra were calculated using density functional theory

(B3LYP) coupled with the 6-31+G* basis set [16][17] implemented in the Gaussian 16 program [18]. This computational method has been shown to often be sufficient for an assignment of the experimental spectra. A scale factor of 0.976 was applied to all the calculated IR spectra, which were also convoluted with 1% of the photon energy to match the FELIX bandwidth.

Results

The products arising from the electrical discharge of pure naphthalene ($m/z = 128$) have been previously investigated using IR-UV mass-selective ion dip spectroscopy [14]. To ease the identification of the new discharge species that form when acetonitrile is added as an additional precursor, we compared the time-of-flight spectrum of the discharge of naphthalene and acetonitrile with a time-of-flight spectrum of the discharge of pure naphthalene in Figure 2. Both spectra exhibit peaks at $m/z < 128$ and $m/z > 128$, corresponding to species arising from fragmentation and recombination chemistry, respectively. As expected, there are several peaks in common between the two mass spectra, namely $m/z = 126, 141, 150, 152, 176$, and 178 , which were already assigned to specific molecular structures in the discharge of pure naphthalene [14]. The experimental IR spectra of the species in common between the two experiments and their assignments are reported in the supplementary information (Figure S1-S6). Several new peaks corresponding to $m/z = 140, 142, 151, 153$, and 167 are observed in the mass spectrum with acetonitrile added as a precursor. The two time-of-flight spectra also differ in the most prominent discharge product, being $m/z = 153$ and $m/z = 141$ in the electrical discharges of naphthalene and acetonitrile and of pure naphthalene, respectively.

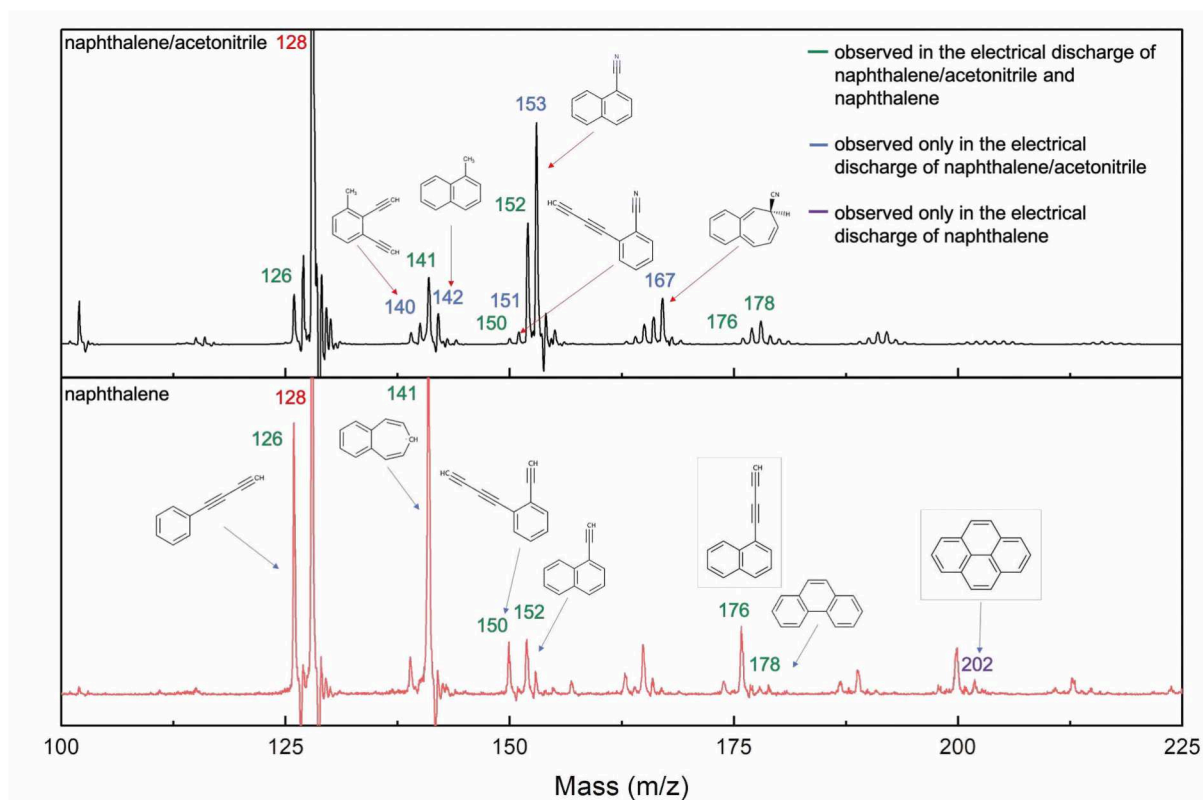


Figure 2 Comparison of the mass spectra of the products of the electrical discharge of naphthalene and acetonitrile (upper trace in black) and of the electrical discharge of pure naphthalene (lower trace in red) highlighting the similarities and differences in produced species between the two experiments. Both mass spectra were obtained via two-colour REMPI (270 nm + 193 nm). The signal at $m/z = 128$, corresponding to the parent species, is truncated in both spectra to improve the visualization of the lower intensity signals. Only the m/z values that are assigned to a specific molecular structure are indicated. The values reported in green, blue, and violet indicate the m/z of species identified in both discharge experiments, only in the discharge experiment of naphthalene and acetonitrile, and only in the discharge experiment of pure naphthalene, respectively. The molecular structure of a representative of the new identified families is also showcased.

The knowledge of the m/z values is often not sufficient to assign the respective molecular structure, especially those of large molecules with an increased diversity of possible species, which are more difficult to differentiate. In order to obtain structural information for the different mass channels, spectroscopic information is therefore needed. We have used a combination of mass-selective IR-UV ion-dip spectroscopy in the $550 - 1800 \text{ cm}^{-1}$ region with quantum-chemical calculations. The assignment is achieved by computing vibrational spectra corresponding to several possible isomers of a certain mass and comparing them with the experimental IR spectrum as shown in Figure 3 for $m/z = 142$ and Figure 4 for $m/z = 153$. Following our chemical intuition and knowing that under electrical discharge conditions acetonitrile is a source of the radicals CN and CH_3 [19], the assignment of $m/z = 142$ and $m/z = 153$ to 1- and 2-methylnaphthalene and 1- and 2-cyanonaphthalene, respectively, was straightforward (Figure 3 and Figure 4). Note that the relative abundance of the isomers is not reflected in the

observed intensity. The latter depends on the excitation and ionization cross section, which can vary depending on the probed molecular species. Both experimental IR spectra corresponding to the mass channels 142 and 153 exhibit vibrational bands in the spectral region between 750 cm^{-1} and 850 cm^{-1} , which are generated by the hydrogen out-of-plane bending motion of substituted aromatic rings. The frequencies of these vibrational bands depend on the position of the substituted aromatic carbon, and this explains the similarities in vibrational frequencies between the vibrational spectra of 1-methylnaphthalene and 1-cyanonaphthalene as well as between the vibrational spectra of 2-methylnaphthalene and 2-cyanonaphthalene.

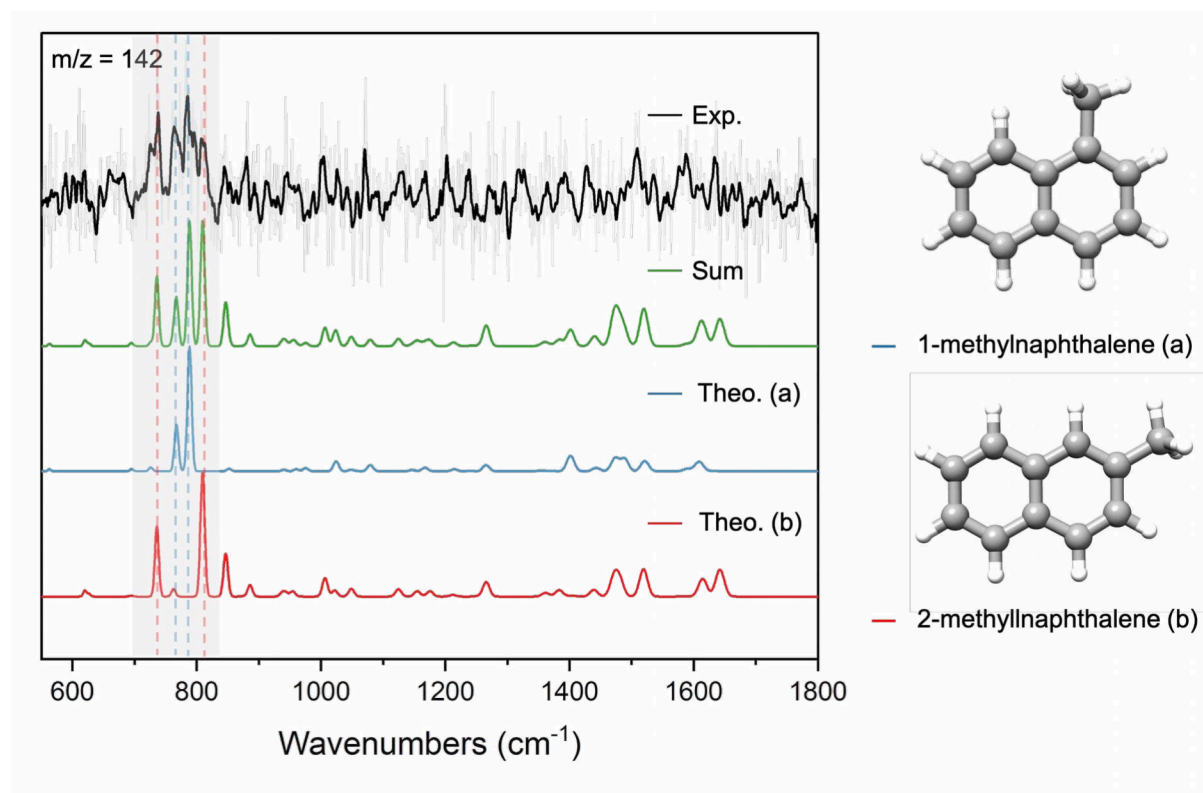


Figure 3 Comparison of the experimental IR spectrum (black trace) recorded in the $550\text{--}1800\text{ cm}^{-1}$ region for $m/z = 142$ with the theoretical vibrational spectra calculated at the B3LYP/6-31+G* level of theory for the two isomers 1-methylnaphthalene (blue trace) and 2-methylnaphthalene (red trace). The trace in light gray represents the average of the experimental IR spectra. The black trace shows the averaged experimental IR spectrum after applying a 5-point adjacent-average smooth function. The green trace provides the sum of the calculated spectra of the two isomers. The shaded areas and the dashed lines highlight the matching features between the experimental and the theoretical vibrational spectra. A scale factor of 0.976 was applied to the theoretical spectra.

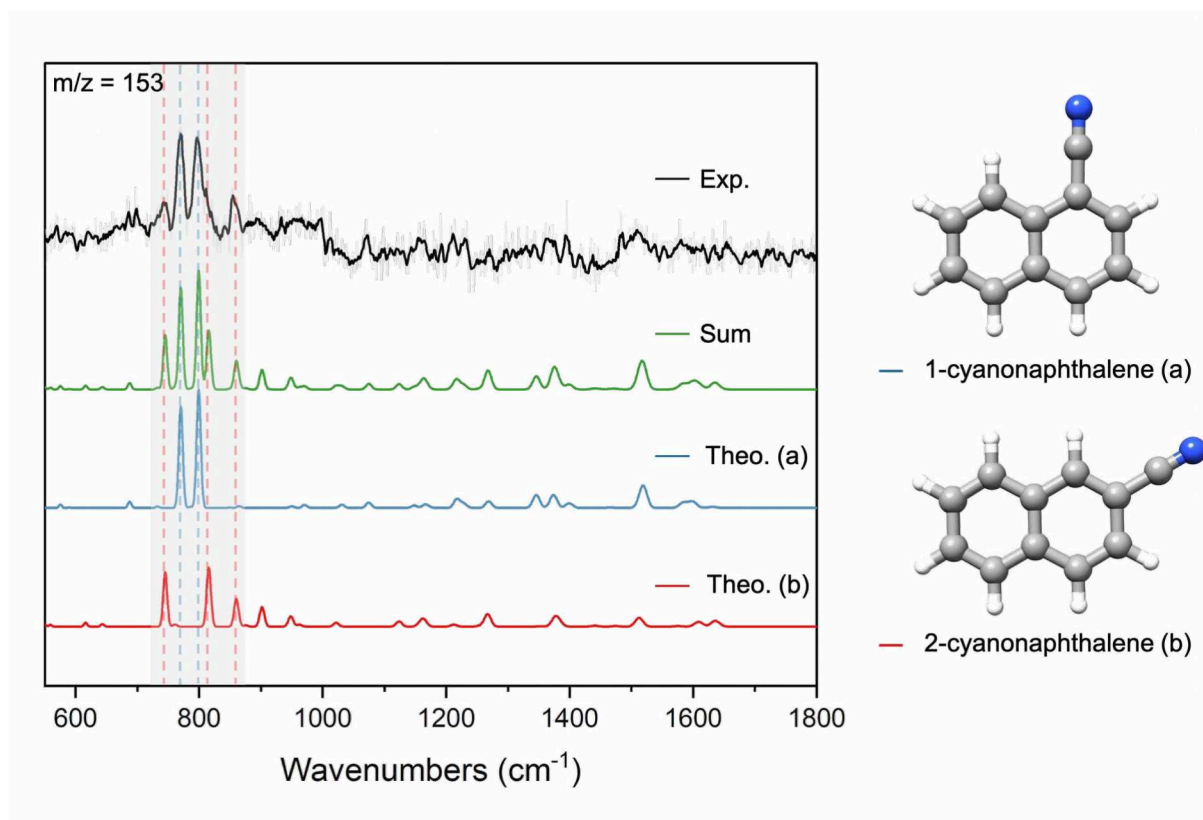


Figure 4 Comparison of the experimental IR spectrum (black trace) recorded in the 550 -1800 cm^{-1} frequency region for $m/z = 153$ with the theoretical vibrational spectra calculated at the B3LYP/6-31+G* for the two isomers 1-cyanonaphthalene (blue trace) and 2-cyanonaphthalene (red trace). The trace in light gray represents the average of the experimental IR spectra. The black trace shows the averaged experimental IR spectrum after applying a 5-point adjacent-average smooth function. The green trace provides the sum of the calculated spectra of the two isomers. The shaded area and the dashed lines highlight the matching features between the experimental and the theoretical vibrational spectra. A scale factor of 0.976 was applied to the theoretical spectra. To better match the experimental spectrum, the theoretical spectra of 1- and 2-cyanonaphthalene have been combined with a 2:1 ratio, respectively.

The IR spectrum corresponding to $m/z = 140$ exhibits a variety of vibrational features along the frequency range investigated (Figure 5). The presence of an intense vibrational band at 1210 cm^{-1} immediately suggested that at least one of the molecules contributing to the experimental IR spectrum should contain a terminal $\text{-C}\equiv\text{C-H}$ group. This band is known to be the result of an overtone generated by the $\equiv\text{C-H}$ bending motion, and it is considered as a diagnostic band for the identification of $\text{-C}\equiv\text{C-H}$ containing structures [20][21]. We have considered a series of isomers containing a $\text{-C}\equiv\text{C-H}$ terminal group in their molecular structure with a $m/z = 140$, which are given at the right-hand side of Figure 5, namely 1-(buta-1,3-diyn-1-yl)-2-methylbenzene (a), 1-(buta-1,3-diyn-1-yl)-3-methylbenzene (b), 1-(buta-1,3-diyn-1-yl)-4-methylbenzene (c), 1,2-diethynyl-3-methylbenzene (d), 1,2-diethynyl-4-methylbenzene (e), 1,3-diethynyl-2-methylbenzene (f), 1,3-diethynyl-5-methylbenzene (g). Their vibrational spectra have been calculated and compared with the experimental IR

spectrum, as shown in Figure 5. All of them exhibit a similar vibrational spectrum with the most intense bands falling in the 600 – 800 cm^{-1} region. The combination of their theoretical vibrational spectra, represented by the light green trace in Figure 5, matches well the frequency region 600 – 800 cm^{-1} . The bands observed around 600 cm^{-1} arise from the out-of-plane deformation of the $\text{-C}\equiv\text{C-H}$ terminal group. These bands are also present in the experimental IR spectra recorded for mass channels 126, 150 and 152, which were assigned to a series of compounds featuring a terminal $\text{-C}\equiv\text{C-H}$ group in their molecular structure (Figure S1, S3 and S4) in the electrical discharge of pure naphthalene. The bands around 800 cm^{-1} are characteristic of aromatic rings and are generated by the CH out-of-plane bending motion. Those around 1400 cm^{-1} are diagnostic of methyl substituted aromatic rings. However, since most of the isomers show similar vibrational features due to their structural similarities, we cannot ensure that all of them are produced in our discharge experiment and in which relative ratios.

Note that, despite the presence of the $\text{-C}\equiv\text{C-H}$ terminal group in all the considered structures, the band at 1210 cm^{-1} does not appear in their theoretical vibrational spectra because the use of anharmonic theory would be required for its correct prediction [22]. Other peaks, mainly in the region 800 - 1000 cm^{-1} and 1200 - 1300 cm^{-1} , are not predicted in any of the calculated spectra. These unaccounted peaks are the result of overtones and combination bands, which make the assignment of the spectrum to a specific structure more complicated. For a clear assignment of the vibrational spectrum, anharmonic frequency calculations as well as experiments employing spectroscopic techniques, such as IR-IR spectroscopy or microwave spectroscopy would be needed. Other isomers of $m/z = 140$, such as 2-ethynyl-1H-indene and cyclopropanaphthalene, were also considered but were discarded as possible contributors due to the absence of their most intense bands in the experimental IR spectrum (Figure S7).

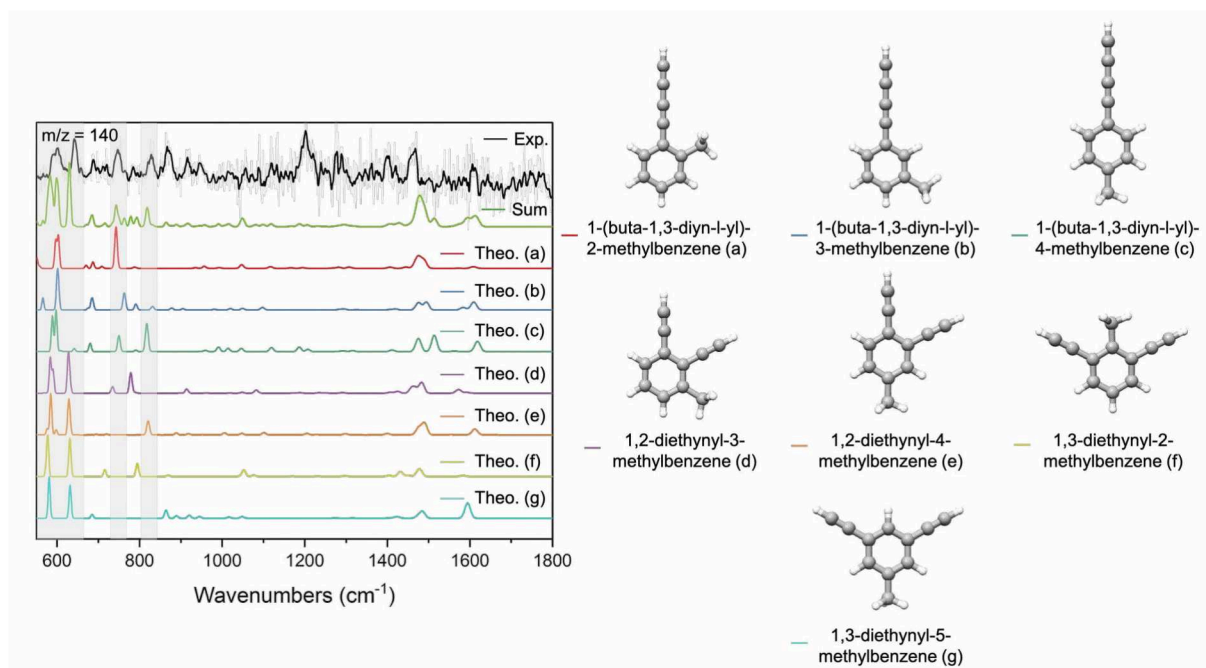


Figure 5 Comparison of the experimental IR spectrum (black trace) recorded in the 550 – 1800 cm^{-1} frequency region for $m/z = 140$ with the theoretical vibrational spectra calculated at the B3YP/6-31+G* level of theory for several isomers (left). The trace in light gray shows the average of the experimental IR spectra. The black trace represents the averaged experimental IR spectrum after applying a 5-point adjacent-average smooth function. The colored traces provide the theoretical vibrational spectra calculated for the molecular structures given on the right-hand side of the figure (a-h). The shaded areas highlight the matching features between the experimental and the theoretical vibrational spectra. A scale factor of 0.976 was applied to the theoretical spectra.

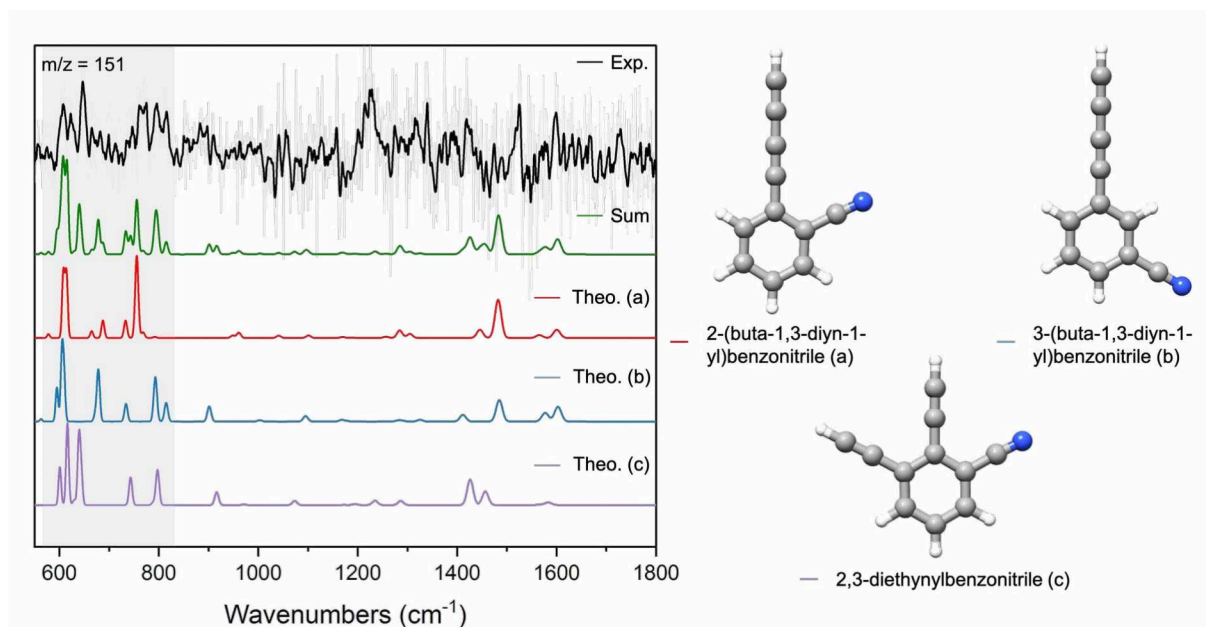


Figure 6 Comparison of the experimental IR spectrum (black trace) recorded in the 550 -1800 cm^{-1} frequency region for $m/z = 151$ with the theoretical vibrational spectra calculated at the B3LYP/6-31+G* level of theory for the three isomers 2-(buta-1,3-diyn-1-yl)benzonitrile (red trace), 3-(buta-1,3-diyn-1-yl)benzonitrile (blue trace), and 2,3-diethynylbenzonitrile (violet trace). The trace in light gray represents the average of the experimental IR spectra. The black trace represents the averaged experimental IR spectrum after applying a 5-point adjacent-average smooth function. The green trace represents the sum of the calculated spectra of the three isomers. The shaded

areas highlight the matching features between the experimental and the theoretical rotational spectra. A scale factor of 0.976 was applied to the theoretical spectra.

The spectrum corresponding to $m/z = 151$ was assigned to a mixture of the three isomers: 2-(buta-1,3-diyn-1-yl)benzonitrile, 3-(buta-1,3-diyn-1-yl)benzonitrile, and 2,3-diethynylbenzonitrile. This assignment was also confirmed by the presence of the vibrational bands at 1210 cm^{-1} in the experimental IR spectrum, which, as mentioned before, is an overtone generated by the $\equiv\text{C-H}$ bending motion and characteristic of molecules featuring a $-\text{C}\equiv\text{C-H}$ terminal group (Figure 6). Other species of $m/z = 151$, which could have formed upon ring opening of naphthalene, such as 5-phenylpenta-2,4-diynenitrile, were also considered as possible reaction products but they were excluded due to a mismatch of their theoretical spectra with the experimental data (Figure S8).

The experimental IR spectrum corresponding to $m/z = 167$ was assigned to the equatorial and axial conformers of the benzo[7]annulene-6-carbonitrile. The combination of their theoretical IR spectra was found to be in good agreement with the experimental data and to match well the region of the experimental IR spectrum between 700 cm^{-1} and 900 cm^{-1} (Figure 7). The experimental IR spectrum exhibits three main vibrational bands, two fall in the range $\sim 730 - 740\text{ cm}^{-1}$ and arise from the CH out-of-plane wagging motion also involving an out-of-plane deformation of the ring, and one at $\sim 800\text{ cm}^{-1}$, generated by the CH out-of-plane bending motion. Due to the similarities between the calculated vibrational spectra of the two conformers of benzo[7]annulene-6-carbonitrile, we could not discriminate between the two species. The seven-membered ring of benzo[7]annulene has three non-equivalent carbon atoms. The theoretical IR spectra of the axial and equatorial conformers of benzo[7]annulene-5-carbonitrile and benzo[7]annulene-7-carbonitrile have also been considered, and a comparison with the experimental IR spectrum is reported in Figure S9, which does not provide a promising agreement.

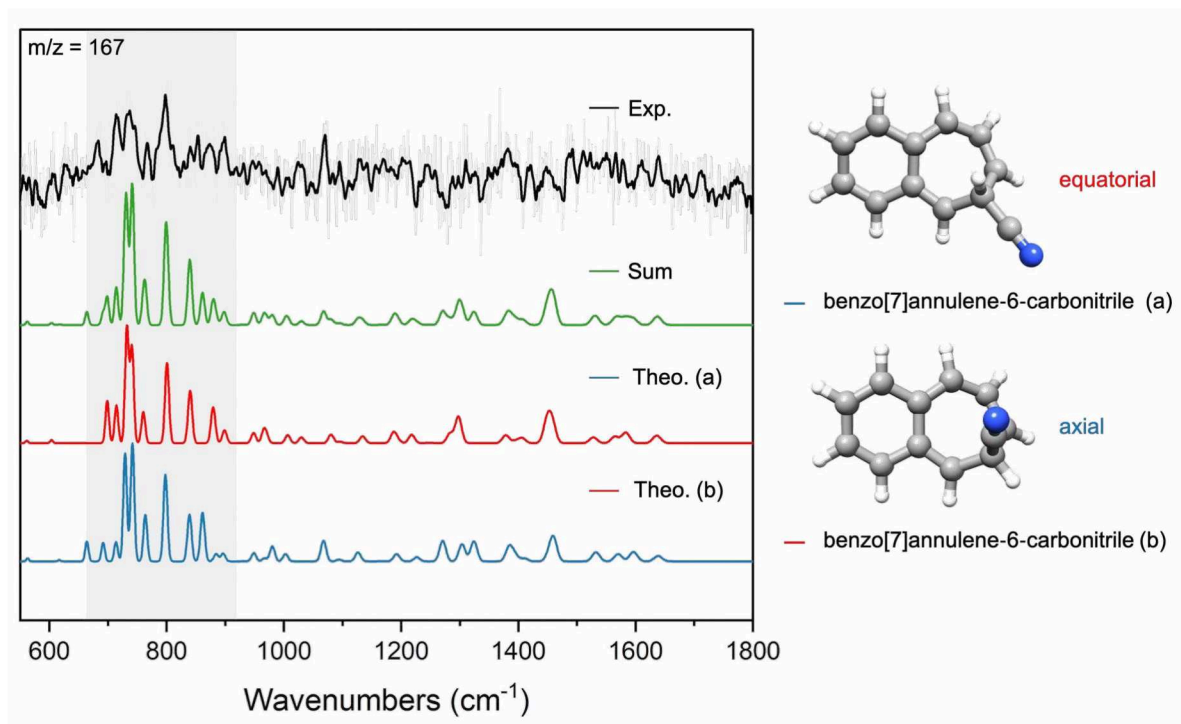


Figure 7 Comparison of the experimental IR spectrum (black trace) recorded in the 550 -1800 cm^{-1} frequency region for $m/z = 167$ with the theoretical vibrational spectra calculated at the B3LYP/6-31+G* level of theory for the two conformers equatorial (red trace) and axial (blue trace) of the benzo[7]annulene-6-carbonitrile. The black trace shows the experimental IR spectrum after applying a 5-point adjacent-average smooth function. The trace in light gray represents the average of the experimental IR spectra. The green trace provides the sum of the calculated spectra of the two conformers. The shaded area highlights the matching features between the experimental and the theoretical vibrational spectra.

Discussion

In general, the outcome of a rich chemistry is observed when a mixture of naphthalene and acetonitrile undergoes electrical discharge. In the experiment of pure naphthalene [14], the formation of two types of PAHs was observed. These included larger PAHs and polyyne-substituted PAHs. With acetonitrile as an additional precursor, we can distinguish between two new classes of PAHs, namely carbonitrile ($-\text{CN}$) and methyl ($-\text{CH}_3$) substituted PAHs.

Several IR spectra presented in this work have been assigned to multiple isomers. Although some isomers could be excluded based on a poor agreement between the calculated and experimental spectra, a unique assignment at this stage resulted to be particularly challenging. This is mostly due to the relatively poor-quality of some of the spectra as they have a relatively low signal-to-noise ratio, as well as to an overlapping of the signature of the possible isomers. From a theoretical point of view, an unambiguous assignment of the spectra could be

assisted by anharmonic vibrational calculations to assign overtones and combination bands. From an experimental point of view, experiments in the far-IR region would allow for the measurement of higher-resolution spectra but also, as already mentioned above, IR-IR spectroscopy or microwave spectroscopy experiments would allow for an unequivocal isomeric discrimination.

A quantitative analysis of the relative amounts of the observed species is complicated due to the spectral dependence on the excitation and ionization cross section of the molecular species; therefore, in the following, we discuss some qualitative observations.

The peak at $m/z = 153$ is the most intense in the mass spectrum, which could indicate that the two isomers 1-cyanonaphthalene and 2-cyanonaphthalene are the dominant species observed in our discharge experiment. The formation of these molecules is expected to take place via a neutral-radical reaction between the PAH naphthalene and the radical CN. Reactions occurring between unsaturated hydrocarbons and the CN radical are, indeed, known to be generally exothermic and barrierless [23][24] [25]. This was shown, for example, in the electrical discharge study of benzene and acetonitrile, which yielded in the formation of benzonitrile [26]. A schematic of the reaction mechanism leading to the formation of cyanonaphthalene is illustrated in Figure 8. Note that the two isomers 1- and 2-cyanonaphthalene have been recently detected in the cold molecular cloud TMC-1 via radio-astronomy and proposed as observational proxies for the parent hydrocarbon naphthalene [4]. The astronomical and laboratory observations of these molecules further emphasize the use of electrical discharge as a powerful experimental tool to produce astronomically relevant species. The two isomers 1- and 2-methylnaphthalene are likely to be formed via a similar neutral-radical reaction pathway as for the cyanonaphthalene (Figure 8). However, we expect the detection of these species via radio astronomy to be challenging due to their relatively low electric dipole moments of 0.3 and 0.5 Debye for 1-methylnaphthalene and 2-methylnaphthalene, respectively.

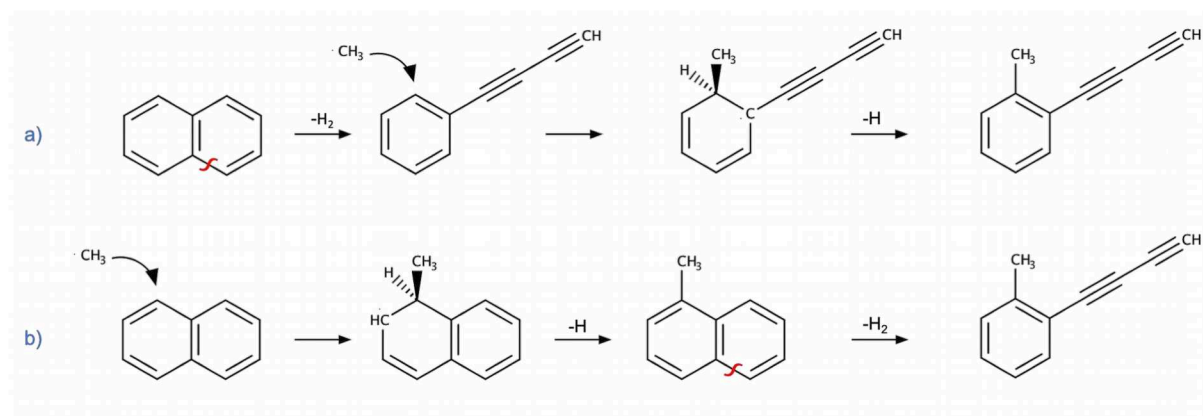


Figure 8 Proposed reaction mechanisms for the formation of 1-cyanonaphthalene (a) and 1-methylnaphthalene (b).

The peak in the mass spectrum at $m/z = 140$ was partially assigned to a series of methyl substituted diacetylene and diethynyl benzene, which could form upon ring opening of the precursors naphthalene or methylnaphthalene. We can indeed propose two formation routes to explain the observation of some of these species, since both naphthalene ($m/z = 128$) and methylnaphthalene ($m/z = 142$) are known to be present in our experiment. If we consider 1-(buta-1,3-diyn-1-yl)-2-methylbenzene, this species could form via a two-step reaction mechanism involving first a C-C cleavage to form diacetylenebenzene, also identified as $m/z = 126$ in our experiment (Figure S1 of the SI), and then a reaction of diacetylenebenzene with the CH₃ radical when starting with naphthalene as the precursor (Figure 9a). Alternatively, methylnaphthalene could form first, via a neutral-radical reaction between naphthalene and the CH₃ radical, to then undergo C-C rupture to produce 1-(buta-1,3-diyn-1-yl)-2-methylbenzene (Figure 9b). Since both diacetylenebenzene ($m/z = 126$) and methylbenzene ($m/z = 142$) have been assigned in our experiment, both proposed mechanisms should be taken into consideration.

As previously mentioned, a discrimination between the species assigned to $m/z = 140$ is not possible due to their similar vibrational spectra. However, most of them have a substantial predicted dipole moment, thus suggesting that an unambiguous assignment of these species could be possible by microwave spectroscopy, a spectroscopic technique which is extremely sensitive to small structural differences, with a parallel study underway in the Hamburg group.

A similar reaction pathway to $m/z = 140$, this time involving the CN radical instead of the CH₃ radical, can also explain the observation of the species having a mass-to-charge ratio of 151, which was assigned to a series of carbonitrile-substituted diethynyl and diacetylene benzene.

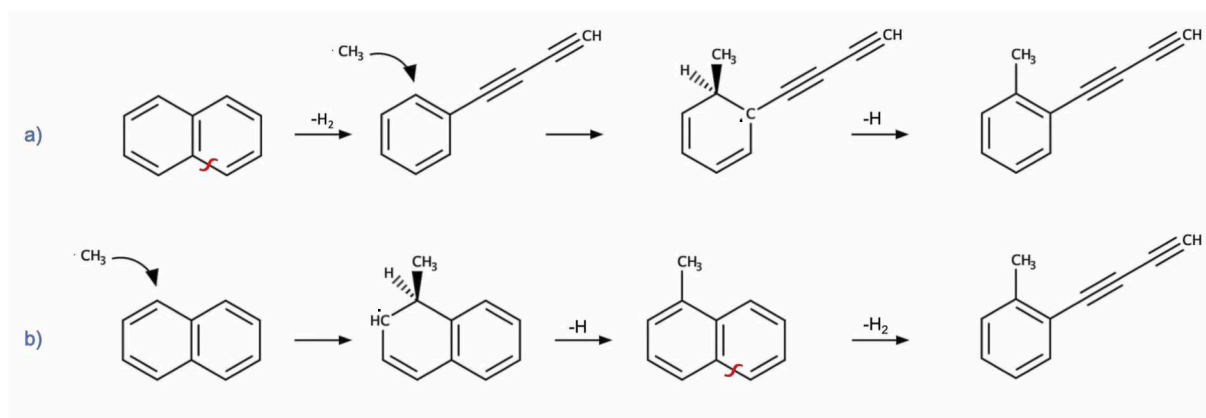


Figure 9 Two proposed two-step reaction mechanisms for the formation of 1-(buta-1,3-dien-1-yl)-2-methylbenzene. a) Reaction mechanism involving first the formation of diacetylenebenzene ($m/z = 126$) and subsequent reaction with the methyl radical. b) Reaction mechanism starting with the neutral-radical reaction between naphthalene and the methyl radical and subsequent C-C cleavage of one of the aromatic rings.

The two conformers of benzo[7]annulene-6-carbonitrile ($m/z = 167$) are thought to be the result of a radical-radical reaction occurring between the radical $-CN$ and the resonance-stabilized radical benzo[7]annulene ($m/z = 141$), which is known to form when naphthalene is subjected to electrical discharge [14] (Figure S2).

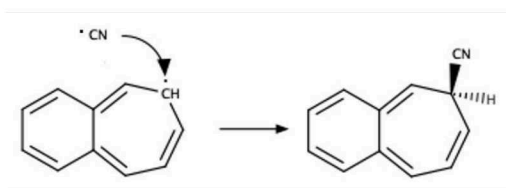


Figure 10 Proposed radical-radical reaction mechanism between the benzo[7]annulene radical and the cyano radical leading to the formation of benzo[7]annulene-6-carbonitrile.

Conclusions

Our experiment elucidates the chemistry that the naphthalene/acetonitrile mixture undergoes when subjected to the harsh energetic conditions generated by an electrical discharge source. In this work, among the carbon chain substituted unsaturated hydrocarbons observed, new $-CN$ and $-CH_3$ substituted species have been identified. Most of these species, especially those containing a nitrogen atom in their molecular structure, such as the benzo[7]annulene-6-carbonitrile, have substantial dipole moments and, therefore, represent good candidates for astronomical observation in interstellar regions, such as the dark molecular cloud TMC-1, where CN-functionalized rings, including benzonitrile

[27], 1-, and 2-cyano-1,3-cyclopentadiene [28], and 1- and 2-cyanonaphthalene [4], have been already discovered.

The use of electrical discharge sources as a way of making new species has been previously shown to create astronomically relevant species [29] [30] [31]. With the observation of the two isomers of cyanonaphthalene in our experiment, we further highlight that this also holds true for PAHs like molecules, which, nowadays, represent one of the main targets of astronomical searches.

To unambiguously confirm the assignment of the observed species, we have recently investigated the electrical discharge chemistry of the naphthalene/acetonitrile mixture using microwave spectroscopy as a complementary experiment. These experiments will be particularly useful to disentangle the different isomers with $m/z=140$ and 167 , which will be nicely distinguished with rotational spectroscopy because of their sufficient electric dipole moments.

Acknowledgments

This work is supported via the ERC starting grant ‘ASTROROT’ (grant number 638027). D.L. was supported by the Alexander von Humboldt fellowship. We would like to thank the FELIX laboratory team for their experimental assistance and we acknowledge the Nederlandse Organisatie voor Wetenschappelijk Onderzoek (NWO) for the support of the FELIX laboratory. The research leading to this result has been supported by the project CALIPSOplus under the Grant Agreement 730872 from the EU Framework Programme for Research and Innovation HORIZON 2020.

Keywords

PAHs, astrochemistry, plasma chemistry, mid-IR, FELs, mass spectrometry, IR-UV spectroscopy

Competing interest

The authors declare no competing interest.

References

- [1] A. G. G. M. Tielens, “Interstellar Polycyclic Aromatic Hydrocarbon Molecules,” *Annual Review of Astronomy and Astrophysics*, vol. 46, no. 1, pp. 289–337, 2008, doi: 10.1146/annurev.astro.46.060407.145211.

- [2] J. Cernicharo *et al.*, "Pure hydrocarbon cycles in TMC-1: Discovery of ethynyl cyclopropenylidene, cyclopentadiene, and indene," *A&A*, vol. 649, p. L15, May 2021, doi: 10.1051/0004-6361/202141156.
- [3] A. M. Burkhardt *et al.*, "Discovery of the Pure Polycyclic Aromatic Hydrocarbon Indene (c-C₉H₈) with GOTHAM Observations of TMC-1," *ApJL*, vol. 913, no. 2, p. L18, May 2021, doi: 10.3847/2041-8213/abfd3a.
- [4] B. A. McGuire *et al.*, "Detection of two interstellar polycyclic aromatic hydrocarbons via spectral matched filtering," *Science*, vol. 371, no. 6535, pp. 1265–1269, Mar. 2021, doi: 10.1126/science.abb7535.
- [5] J. Zhen, P. Castellanos, D. M. Paardekooper, H. Linnartz, and A. G. G. M. Tielens, "Laboratory Formation of Fullerenes from PAHs: Top-down Interstellar Chemistry," *The Astrophysical Journal*, vol. 797, p. L30, Dec. 2014, doi: 10.1088/2041-8205/797/2/L30.
- [6] O. Berné, J. Montillaud, and C. Joblin, "Top-down formation of fullerenes in the interstellar medium," *A&A*, vol. 577, p. A133, May 2015, doi: 10.1051/0004-6361/201425338.
- [7] M. Frenklach, "Reaction mechanism of soot formation in flames," *Phys. Chem. Chem. Phys.*, vol. 4, no. 11, pp. 2028–2037, May 2002, doi: 10.1039/B110045A.
- [8] R. K. E. Gover, T. W. Chamberlain, P. J. Sarre, and A. N. Khlobystov, "Piecing Together Large Polycyclic Aromatic Hydrocarbons and Fullerenes: A Combined ChemTEM Imaging and MALDI-ToF Mass Spectrometry Approach," *Frontiers in Chemistry*, vol. 9, p. 425, 2021, doi: 10.3389/fchem.2021.700562.
- [9] A. M. Rijs, M. Kabeláč, A. Abo-Riziq, P. Hobza, and M. S. de Vries, "Isolated Gramicidin Peptides Probed by IR Spectroscopy," *ChemPhysChem*, vol. 12, no. 10, pp. 1816–1821, 2011, doi: 10.1002/cphc.201100212.
- [10] A. K. Lemmens, D. B. Rap, J. M. M. Thunnissen, B. Willemsen, and A. M. Rijs, "Polycyclic aromatic hydrocarbon formation chemistry in a plasma jet revealed by IR-UV action spectroscopy," *Nature Communications*, vol. 11, no. 1, Art. no. 1, Jan. 2020, doi: 10.1038/s41467-019-14092-3.
- [11] A. J. Remijan, J. M. Hollis, F. J. Lovas, D. F. Plusquellic, and P. R. Jewell, "Interstellar Isomers: The Importance of Bonding Energy Differences," *ApJ*, vol. 632, no. 1, p. 333, Oct. 2005, doi: 10.1086/432908.
- [12] K. I. Öberg *et al.*, "The comet-like composition of a protoplanetary disk as revealed by complex cyanides," *Nature*, vol. 520, no. 7546, pp. 198–201, Apr. 2015, doi: 10.1038/nature14276.
- [13] Y. C. Minh, W. M. Irvine, M. Ohishi, S. Ishikawa, S. Saito, and N. Kaifu, "Measurement of the methyl cyanide E/A ratio in TMC-1," *Astron Astrophys*, vol. 267, pp. 229–232, 1993.
- [14] A. K. Lemmens, D. B. Rap, J. M. M. Thunnissen, B. Willemsen, and A. M. Rijs, "Polycyclic aromatic hydrocarbon formation chemistry in a plasma jet revealed by IR-UV action spectroscopy," *Nature Communications*, vol. 11, no. 1, p. 269, Jan. 2020, doi: 10.1038/s41467-019-14092-3.
- [15] D. Oepts, A. F. G. van der Meer, and P. W. van Amersfoort, "The Free-Electron-Laser user facility FELIX," *Infrared Physics & Technology*, vol. 36, no. 1, pp. 297–308, Jan. 1995, doi: 10.1016/1350-4495(94)00074-U.
- [16] A. D. Becke, "Density-functional thermochemistry. III. The role of exact exchange," *J. Chem. Phys.*, vol. 98, no. 7, pp. 5648–5652, Apr. 1993, doi: 10.1063/1.464913.
- [17] C. Lee, W. Yang, and R. G. Parr, "Development of the Colle-Salvetti correlation-energy formula into a functional of the electron density," *Phys. Rev. B*, vol. 37, no. 2, pp. 785–789, Jan. 1988, doi: 10.1103/PhysRevB.37.785.
- [18] Frisch, M. J. G. *et al.*, *Gaussian 16, Revision A.03*. Gaussian, Inc., Wallingford CT, 2016.

- [19] P. Li and W. Y. Fan, "The CN free radical in acetonitrile discharges," *Journal of Applied Physics*, vol. 93, no. 12, pp. 9497–9502, Jun. 2003, doi: 10.1063/1.1575928.
- [20] R. A. Nyquist and W. J. Potts, "Infrared absorptions characteristic of the terminal acetylenic group ($-C\equiv C-H$)," *Spectrochimica Acta*, vol. 16, no. 4, pp. 419–427, Jan. 1960, doi: 10.1016/0371-1951(60)80036-7.
- [21] J. C. Evans and R. A. Nyquist, "The vibrational spectra and vibrational assignments of the propargyl halides," *Spectrochimica Acta*, vol. 19, no. 7, pp. 1153–1163, Jul. 1963, doi: 10.1016/0371-1951(63)80035-1.
- [22] P. Constantinidis, F. Hirsch, I. Fischer, A. Dey, and A. M. Rijs, "Products of the Propargyl Self-Reaction at High Temperatures Investigated by IR/UV Ion Dip Spectroscopy," *ACS Publications*, Dec. 20, 2016. <https://pubs.acs.org/doi/pdf/10.1021/acs.jpca.6b08750> (accessed Oct. 26, 2021).
- [23] N. Balucani *et al.*, "Crossed beam reaction of cyano radicals with hydrocarbon molecules. I. Chemical dynamics of cyanobenzene (C_6H_5CN ; X1A1) and perdeutero cyanobenzene (C_6D_5CN ; X1A1) formation from reaction of $CN(X^2\Sigma^+)$ with benzene $C_6H_6(X1A1g)$, and d6-benzene $C_6D_6(X1A1g)$," *J. Chem. Phys.*, vol. 111, no. 16, pp. 7457–7471, Oct. 1999, doi: 10.1063/1.480070.
- [24] C. J. Bennett *et al.*, "A chemical dynamics, kinetics, and theoretical study on the reaction of the cyano radical (CN ; $X^2\Sigma^+$) with phenylacetylene (C_6H_5CCH ; X1A1)," *Phys. Chem. Chem. Phys.*, vol. 12, no. 31, pp. 8737–8749, Jul. 2010, doi: 10.1039/B925072G.
- [25] I. R. Cooke, D. Gupta, J. P. Messinger, and I. R. Sims, "Benzonitrile as a Proxy for Benzene in the Cold ISM: Low-temperature Rate Coefficients for $CN + C_6H_6$," *ApJL*, vol. 891, no. 2, p. L41, Mar. 2020, doi: 10.3847/2041-8213/ab7a9c.
- [26] K. L. K. Lee, B. A. McGuire, and M. C. McCarthy, "Gas-phase synthetic pathways to benzene and benzonitrile: a combined microwave and thermochemical investigation," *Phys. Chem. Chem. Phys.*, vol. 21, no. 6, pp. 2946–2956, Feb. 2019, doi: 10.1039/C8CP06070C.
- [27] B. A. McGuire *et al.*, "Detection of the aromatic molecule benzonitrile ($c-C_6H_5CN$) in the interstellar medium," *Science*, vol. 359, no. 6372, pp. 202–205, Jan. 2018, doi: 10.1126/science.aao4890.
- [28] M. C. McCarthy *et al.*, "Interstellar detection of the highly polar five-membered ring cyanocyclopentadiene," *Nat Astron*, vol. 5, no. 2, pp. 176–180, Feb. 2021, doi: 10.1038/s41550-020-01213-y.
- [29] M. C. McCarthy, W. Chen, M. J. Travers, and P. Thaddeus, "Microwave Spectra of 11 Polyyne Carbon Chains," *The Astrophysical Journal Supplement Series*, vol. 129, pp. 611–623, Aug. 2000, doi: 10.1086/313428.
- [30] M. C. McCarthy, E. S. Levine, A. J. Apponi, and P. Thaddeus, "Experimental Structures of the Carbon Chains HC_7N , HC_9N , and $HC_{11}N$ by Isotopic Substitution," *Journal of Molecular Spectroscopy*, vol. 203, no. 1, pp. 75–81, Sep. 2000, doi: 10.1006/jmsp.2000.8149.
- [31] M. C. McCarthy *et al.*, "Exhaustive Product Analysis of Three Benzene Discharges by Microwave Spectroscopy," *J. Phys. Chem. A*, vol. 124, no. 25, pp. 5170–5181, Jun. 2020, doi: 10.1021/acs.jpca.0c02919.

